Research Article BEU Fen Bilimleri Dergisi 15(1): 322-327 (2026) DOI: 10.17798/bitlisfen.1804343

BİTLİS EREN UNIVERSITY
FEN BİLİMLERİ DERGİSİ
ISSN: 2147-3129 / e-ISSN: 2147-3188

TUNABLE SECOND-HARMONIC GENERATION IN "4-3" TUNED QUANTUM WELLS DRIVEN BY ELECTRIC FIELDS

Ozan ÖZTÜRK

Sivas Cumhuriyet University, Department of Nanotechnology Engineering, Sivas, Türkiye, ozanozturk@cumhuriyet.edu.tr

Article Info

Received: *October 15, 2025*
Revised: *December 1, 2025*
Accepted: *December 22, 2025*

Keywords
GaAs/AlGaAs quantum wells,
Second-harmonic generation (SHG),
Electric field.

ABSTRACT

In this study, we investigate the influence of external electric fields on the potential profile, energy states, dipole moment matrix elements (DMMEs), and second-harmonic generation (SHG) in the "4-3" GaAs/AlGaAs quantum wells (QWs). By varying the electric field strength, pronounced modifications are observed in electron localization within the coupled wells, accompanied by notable shifts in the energy levels. A transition from an asymmetric to a symmetric potential profile occurs at a critical field of F = 57 kV/cm, leading to an equal distribution of electrons across both wells. The SHG response exhibits a strong dependence on the applied field: a redshift dominates below the critical field, while a blueshift emerges above it, and the SHG coefficient vanishes completely at the symmetric configuration. These results demonstrate that external electric fields provide an effective mechanism for tuning the nonlinear optical properties of the 4-3 QWs, offering potential applications in nano optoelectronic and photonic devices.

1. INTRODUCTION

Quantum wells (QWs) have long served as a fertile platform for exploring and engineering low-dimensional electronic and optical phenomena, thanks to their discrete energy spectra, enhanced quantum confinement, and strong light–matter interactions [1]. By tailoring layer thicknesses, barrier heights, and doping profiles, one can systematically modulate the subband structure, wavefunction overlap, and transition matrix elements, thereby customizing device-level properties such as intersubband absorption, electro-optic modulation, and nonlinear optics [2].

Among the nonlinear optical phenomena, the second-harmonic generation (SHG) coefficient occupies a key position due to its technological relevance (e.g. frequency conversion, optical modulators, wavelength tuning) and its sensitivity to the symmetry properties of the structure [3, 4]. In bulk centrosymmetric semiconductors, SHG is forbidden under the electric-dipole approximation, but in low-dimensional heterostructures the broken inversion symmetry allows a nonzero second-order susceptibility. Thus, asymmetric QWs are a promising architecture to realizing efficient SHG within semiconductor platforms. A further degree of tunability arises when an external electric field is applied across a QW structure. The field can tilt the potential landscape through the quantum-confined Stark effect, shift energy subbands via Stark shifts, modulate carrier localization, and thereby alter transition dipole moments and resonance conditions. In asymmetric wells, this additional flexibility becomes particularly powerful: the applied field can either reinforce or counterbalance the intrinsic structural asymmetry, allowing in-situ, reversible control of SHG magnitude and spectral position [5].

Over the decades, several theoretical and experimental works have explored electric-field–enhanced SHG coefficient in quantum wells. Tsang et al. predicted that applying electric fields of order 10–70 kV/cm can enhance the second-harmonic susceptibility by one to two orders of magnitude in asymmetric QWs relative to bulk GaAs [6]. Zhai et al. studied electric-field–induced SHG coefficient in asymmetric Gaussian-potential wells using the effective mass approximation, observing modulation of SHG intensity with field strength [7]. More recently, Zhang et al. investigated the sensitivity of SHG coefficient to applied fields and structural parameters in nanostructures, reinforcing the idea that field tuning is a promising route to modulate nonlinear optical response [8]. Additionally, Jaouane et al.

investigated the nonlinear optical properties of a single donor dopant in multilayer quantum dots under electric field [9]. Furthermore, a recent study highlighted once again the significant influence of external electric fields and structural parameters on the nonlinear optical response of quantum well systems [10].

In this study, the "4-3" tuned GaAs/GaAlAs QWs under different electric field strengths are investigated to examine the effects of potential asymmetry, energy level shifts, and dipole moment matrix element (DMME) variations on SHG. In particular, it was observed that at the critical electric field, where the potential profile undergoes a symmetry transition, the SHG coefficient exhibits pronounced changes. In previous research, harmonic generation analyses were mainly carried out on the symmetrically designed "12–6" tuned GaAs/AlGaAs double QW structures. For example, Zhang et al. introduced asymmetry into this symmetric configuration by applying an external electric field and subsequently calculated both the SHG and THG coefficients [8]. In contrast, Rodríguez-Magdaleno et al. examined the same "12-6" configuration, which remains symmetric in the absence of an electric field, and therefore reported only the THG coefficient, as the SHG response vanishes in symmetric QWs [11]. To the best of our knowledge, the present study is the first to investigate the inherently asymmetric "4-3" tuned GaAs/GaAlAs QW structure, which can exhibit a non-zero SHG response even without an applied field, clearly distinguishing it from the previously explored "12-6" systems.

2. THEORY

The stationary Hamiltonian describing the GaAs/AlGaAs QW system is presented in Eq. (1). Within the framework of the effective mass approximation, the eigenfunctions and energy spectra are obtained by employing the finite element method (FEM).

$$\mathrm{H} = -\frac{\hbar^2}{2\mathrm{m}^*}\frac{\mathrm{d}^2}{\mathrm{dz}^2} + \mathrm{e\,F\,z} + \mathrm{V(z)} \tag{1}$$

The Hamiltonian includes a second-order differential equation, which is solved through matrix diagonalization [12, 13]. Here, m^* denotes the effective electron mass, e is the elementary charge, F is the applied electric field along the growth axis, and $\mathrm{V(z)}$ represents the confining potential.

$$\mathrm{V(z)} = 4\,\mathrm{V_0}\left\{\left(\frac{\mathrm{z}}{\mathrm{L}}\right)^4 - \left(\frac{\mathrm{z}}{\mathrm{L}}\right)^3\right\} \tag{2}$$

Here, m^*=0.067 $\mathrm{m_0}$ ($\mathrm{m_0}$ being the free electron mass), L =20 nm and $\mathrm{V_0}$=228 meV.

After determining the wave functions and Energy levels, the SHG coefficients are calculated using the compact density matrix approach [14, 15].

$$\chi_{2\omega}^{(2)} = \frac{\mathrm{e}^3\,\sigma_\mathrm{v}}{\varepsilon_\mathrm{o}}\frac{\mathrm{M_{21}M_{32}M_{31}}}{(\hbar\omega - \mathrm{E_{21}} - \mathrm{i}\hbar\Gamma)(2\hbar\omega - \mathrm{E_{31}} - \mathrm{i}\hbar\Gamma/2)} \tag{3}$$

Here, $\mathrm{M_{fi}} = \int \Psi_\mathrm{f}^*\ \mathrm{z}\ \Psi_\mathrm{i}\,\mathrm{dz}$ denotes DMME, ω is the angular frequency of the photon, $\mathrm{E_{fi}} = \mathrm{E_f} - \mathrm{E_i} = \hbar\,\omega_\mathrm{fi}$ represents the transition energy between $\mathrm{E_f}$ and $\mathrm{E_i}$ energy states.

3. RESULTS AND DISCUSSION

We have analyzed the variation of the potential profile and SHG coefficients in 4-3 GaAs/AlGaAs QW structure under F. The parameters used in the calculations are $\mathrm{T} = 1/\Gamma = 0.5$ ps, $\sigma_\mathrm{v} = 3\mathrm{x}10^{22}\mathrm{m}^{-3}$.

Figure 1 illustrates the potential profile under different strengths of the applied F and the corresponding probability distributions of electrons in each energy level. In Figure 1a, for F = 0, the potential is sharper on the right side and shallower on the left side. Electrons at the E_1 energy level are localized on the right, whereas those at the E_2 and E_3 levels are concentrated on the left. When the electric field is increased to F = 20 kV/cm, the potential tilts towards the left, reducing the sharpness on the right side and shifting the energy levels downward. In this case, electrons at the E_2 and E_3 levels spread further into the left region (Figure 1b). At F = 40 kV/cm, the tilting of the potential becomes more pronounced: the right-

hand sharpness decreases further, while the left-hand potential depth increases. Although electrons at the E_1 level remain localized on the right, those at the E_2 level are almost entirely confined to the left (Figure 1c). For F = 60 kV/cm (Figure 1d), the left side of the potential becomes deeper, while the right side becomes shallower. Consequently, electrons in all energy levels begin to distribute across the entire potential, and the dominant localization of electrons at E_1 and E_2 essentially interchanges. The inset graph shows that at F = 57 kV/cm (referred to hereafter as the critical field value), the initially asymmetric potential transforms into a symmetric structure, yielding two identical quantum wells. At this field, electrons at each level are equally distributed between the two wells. When the electric field increases to F = 80 kV/cm, the left well becomes deeper and sharper, while the right well becomes shallower. As a result, electrons at E_1 localize on the left, whereas those at E_2 concentrate on the right (Figure 1e). At F = 100 kV/cm, the potential profile nearly mirrors that of F = 0. In this configuration, electrons at E_2 localize on the right side within a broader region compared to the case without an electric field (Figure 1f).

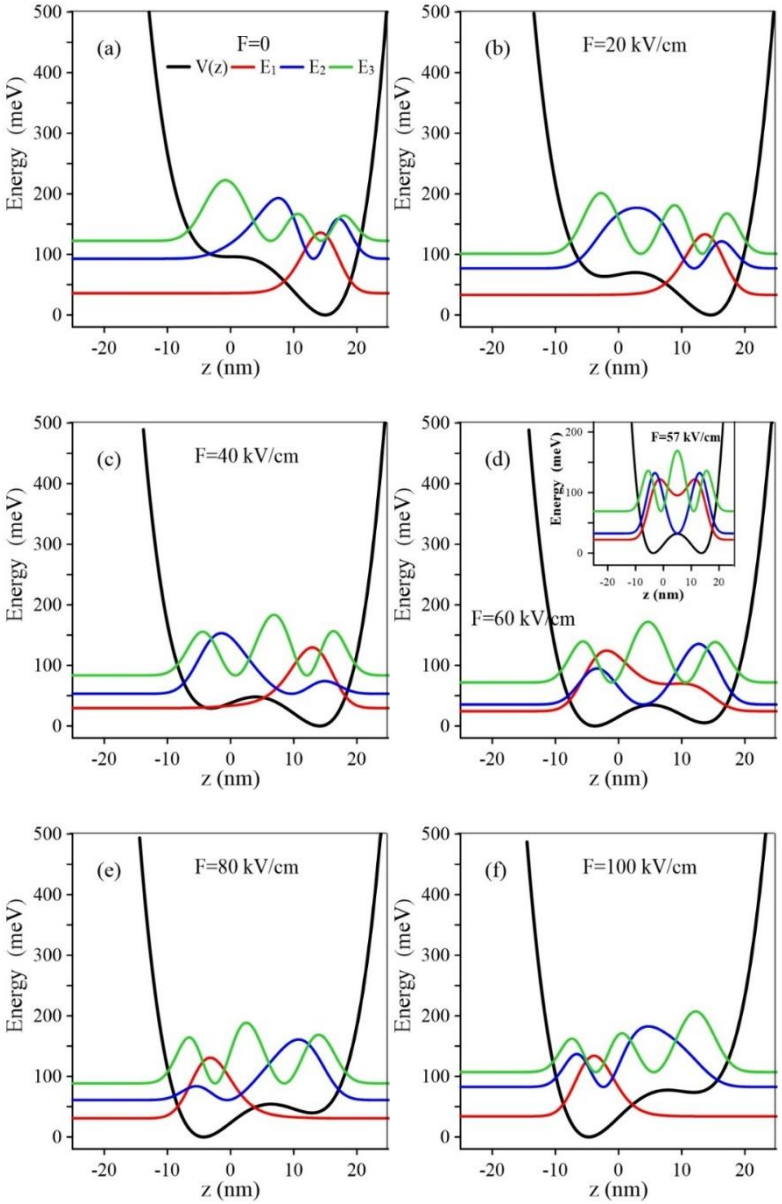

Figure 1. For (a) F=0, (b) F=20 kV/cm, (c) F=40 kV/cm, (d) F=60 kV/cm (inset show for F=57 kV/cm), (e) F=80 kV/cm and (f) F=100 kV/cm, the potential profile and the probability densities of electrons in the first three bound energy states.

Figure 2a shows the variation of the two main energy differences as a function of the applied electric field, while the inset depicts the variation of the first three energy levels. As observed in the inset, the E_1 energy level changes only slightly with increasing F, showing a minor reduction at the critical field. The E_2 and E_3 levels, however, decrease rapidly up to the critical field and then increase sharply beyond this point. Since the most significant variation occurs at E_2, the change in E_{21} is much more pronounced than that of $E_{31}/2$. Both energy differences reach their minimum values at the critical field, and additionally, they coincide at F = 35 kV/cm and F = 80 kV/cm. The product of DMMEs as a function of F is presented in Figure 2b, with the inset showing individual DMMEs. At the critical field, absolute M_{21} exhibits a maximum peak, while absolute M_{31} becomes zero due to symmetry. In contrast, absolute M_{32} is only weakly affected by the electric field. The product of the DMMEs reaches a minimum at the critical field, while displaying oscillatory increases and decreases at other field values.

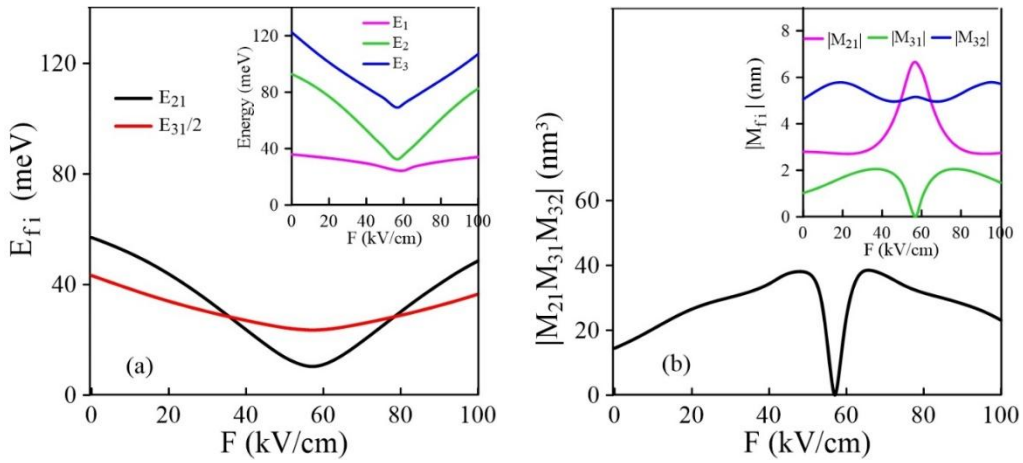

Figure 2. The variations of (a) the energy differences E_{21}, $E_{31}/2$ and (b) the product of DMMEs as functions of the electric field. Insets show (a) the changes of the energy levels and (b) the variations of the DMMEs.

Figure 3 presents the SHG coefficients as a function of photon energy for different electric field strengths. To make all peaks clearly visible, the SHG coefficient at F = 80 kV/cm is reduced by a factor of two. The smaller peaks in the SHG spectra are associated with the E_{21} transition, whereas the larger peaks correspond to the $E_{31}/2$ transition. For F ≤ 35 kV/cm, the smaller peaks appear on the right side of the dominant peak; for 35 < F < 80 kV/cm, they shift to the left side; and for F > 80 kV/cm, they reappear on the right. Up to the critical field, the SHG coefficient exhibits a redshift in the optical spectrum, while beyond this point it shows a blueshift. At the critical field, due to the symmetry of the potential, the SHG coefficient vanishes completely. For F = 40 kV/cm, the E_{21} and $E_{31}/2$ energy differences become nearly degenerate, resulting in a strong SHG peak with a small side peak on the left. The largest single peak emerges at F = 80 kV/cm, where the E_{21} and $E_{31}/2$ transition energies overlap.

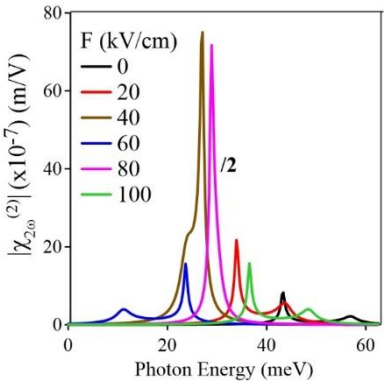

Figure 3. Variations of the SHG coefficient versus photon energy for different values of the electric field.

From these results, it can be concluded that since the shape of the quantum well strongly depends on the applied electric field F, the energy levels, dipole matrix elements, and consequently the SHG coefficients undergo significant modifications. While typical electric field studies on asymmetric Gaussian or step-like wells reported by Tsang et al. [6], Zhai et al. [7], and Altun [16] often demonstrate a monotonic enhancement or modulation of SHG, our "4-3" system exhibits a unique symmetry-restoring transition at a critical field (F=57 kV/cm) where the SHG signal vanishes completely. This behavior highlights a distinct tunability mechanism where the electric field is used not just to induce asymmetry, but to actively tune the system through a perfect symmetry point.

4. CONCLUSION

We have shown that the electronic and optical properties of 4-3 quantum wells can be efficiently controlled by external electric fields. The potential profile and electron localization undergo a transition from an asymmetric to a symmetric structure at the critical field of F = 57 kV/cm, leading to significant changes in energy levels and dipole matrix elements. As a result, the SHG coefficients become strongly dependent on the electric field, and spectral shifts from red to blue are observed. In particular, the vanishing of SHG at the symmetric potential at the critical electric field and the emergence of a large SHG peak at F = 80 kV/cm highlight the sensitivity of nonlinear optical processes to field-induced structural modifications. These findings confirm that 4-3 QWs are promising candidates for tunable nonlinear optical devices, where electric fields can serve as an effective external control parameter.

Statement of Research and Publication Ethics

The study is complied with research and publication ethics.

Artificial Intelligence (AI) Contribution Statement

This manuscript was entirely written, edited, analyzed, and prepared without the assistance of any artificial intelligence (AI) tools. All content, including text, data analysis, and figures, was solely generated by the authors.

REFERENCES

[1] J. Frigerio *et al.*, "Second Harmonic Generation in Germanium Quantum Wells for Nonlinear Silicon Photonics," *ACS Photonics,* vol. 8, no. 12, pp. 3573-3582, 2021.

[2] F. Ungan, M. K. Bahar, J. C. Martinez-Orozco, and M. E. Mora-Ramos, "Optical responses in asymmetric hyperbolic-type quantum wells under the effect of external electromagnetic fields," *Photonics and Nanostructures - Fundamentals and Applications,* vol. 41, p. 100833, 2020.

[3] G. Chesi, V. Falcone, S. Calcaterra, M. Virgilio, and J. Frigerio, "Modelling second harmonic generation at mid-infrared frequencies in waveguide integrated Ge/SiGe quantum wells," *Optics Express,* vol. 31, no. 11, pp. 17098-17111, 2023.

[4] R. Arraoui, M. Jaouane, A. Ed-Dahmouny, A. Fakkahi, K. El-Bakkari, M. N. Murshed, H. E. Ghazi, A. Sali, and N. Zeiri, "Influence of structural factors and impurity position on second harmonic generation in double-quantum box GaAs-Ga1-xAlxAs structures," *The European Physical Journal Plus,* vol. 139, no. 9, p. 830, 2024.

[5] M. J. Karimi and A. Keshavarz, "Second harmonic generation in asymmetric double semi-parabolic quantum wells: Effects of electric and magnetic fields, hydrostatic pressure and temperature," *Physica E: Low-dimensional Systems and Nanostructures,* vol. 44, no. 9, pp. 1900-1904, 2012.

[6] L. Tsang, D. Ahn, and S. L. Chuang, "Electric field control of optical second-harmonic generation in a quantum well," *Applied Physics Letters,* vol. 52, no. 9, pp. 697-699, 1988.

[7] W. Zhai, "A study of electric-field-induced second-harmonic generation in asymmetrical Gaussian potential quantum wells," *Physica B: Condensed Matter,* vol. 454, pp. 50-55, 2014.

[8] Z.-H. Zhang, Z.-Y. Song, J.-H. Yuan, and S.-L. Li, "Effect of electric field on the second- and third-harmonic generation of "12–6" tuned GaAs/AlGaAs double quantum well," *International Journal of Modern Physics B,* vol. 37, no. 18, p. 2350177, 2022.

[9] M. Jaouane, R. Arraoui, A. Fakkahi, A. Ed-Dahmouny, H. Azmi, K. El-Bakkari, J. El-Hamouchi, A. Sali, and F. Ungan, "Nonlinear optical properties of a single donor dopant in multilayered quantum dots under an electric field," *Physica B: Condensed Matter,* vol. 716, p. 417701, 2025.

[10] A. T. Tuzemen, "Effects of external fields and structural parameters on third harmonic generation of GaAs/AlGaAs Manning-like double quantum well structure," *The European Physical Journal Plus,* vol. 139, no. 6, p. 513, 2024.

[11] K. A. Rodríguez-Magdaleno, M. Demir, F. Ungan, F. M. Nava-Maldonado, and J. C. Martínez-Orozco, "Third harmonic generation of a 12–6 GaAs/Ga_{1-x}Al_{x}As double quantum well: effect of external fields," *The European Physical Journal Plus,* vol. 139, no. 4, p. 359, 2024.

[12] D. Altun, O. Ozturk, B. O. Alaydin, and E. Ozturk, "Linear and nonlinear optical properties of a superlattice with periodically increased well width under electric and magnetic fields," *Micro and Nanostructures,* vol. 166, p. 207225, 2022.

[13] K. Nakamura, A. Shimizu, M. Koshiba, and K. Hayata, "Finite-element analysis of quantum wells of arbitrary semiconductors with arbitrary potential profiles," *IEEE Journal of Quantum Electronics,* vol. 25, no. 5, pp. 889-895, 1989.

[14] B. O. Alaydin, D. Altun, O. Ozturk, and E. Ozturk, "High harmonic generations triggered by the intense laser field in GaAs/AlxGa1-xAs honeycomb quantum well wires," *Materials Today Physics,* vol. 38, p. 101232, 2023.

[15] B. O. Alaydin, O. Ozturk, D. Altun, and E. Ozturk, "Coupled cylindrical quantum well wires in broken symmetry: effects of intense laser field on the harmonic generations," *The European Physical Journal Plus,* vol. 139, no. 10, p. 908, 2024.

[16] D. Altun, "Optical rectification and second harmonic generation in different shape GaAs/AlGaAs double quantum wells under electric and magnetic fields," *International Journal of Modern Physics B,* vol. 39, no. 22, p. 2550200, 2025.